Department of Medicine Publications   Medicine Department

1-1-2019

Back to the Basics: Resting State Functional Connectivity of the Reticular Activation System in PTSD and its Dissociative Subtype.

Janine Thome

Maria Densmore

Georgia Koppe

Braeden Terpou

Jean Theberge
The university of Western Ontario, jthberge@uwo.ca

See next page for additional authors

Authors

Janine Thome, Maria Densmore, Georgia Koppe, Braeden Terpou, Jean Theberge, Margaret C McKinnon, and Ruth A Lanius

Back to the Basics: Resting State Functional Connectivity of the Reticular Activation System in PTSD and its Dissociative Subtype

Janine Thome[1,2,3] ![ID], Maria Densmore[1,4], Georgia Koppe[2,3],
Braeden Terpou[1,5] ![ID], Jean Théberge[1,4,6] ![ID],
Margaret C. McKinnon[7,8,9], and Ruth A. Lanius[1,4,5,7]

Abstract

Background: Brainstem and midbrain neuronal circuits that control innate, reflexive responses and arousal are increasingly recognized as central to the neurobiological framework of post-traumatic stress disorder (PTSD). The reticular activation system represents a fundamental neuronal circuit that plays a critical role not only in generating arousal but also in coordinating innate, reflexive responding. Accordingly, the present investigation aims to characterize the resting state functional connectivity of the reticular activation system in PTSD and its dissociative subtype.

Methods: We investigated patterns of resting state functional connectivity of a central node of the reticular activation system, namely, the pedunculopontine nuclei, among individuals with PTSD (n = 77), its dissociative subtype (PTSD+DS; n = 48), and healthy controls (n = 51).

Results: Participants with PTSD and PTSD+DS were characterized by within-group pedunculopontine nuclei resting state functional connectivity to brain regions involved in innate threat processing and arousal modulation (i.e., midbrain, amygdala, ventromedial prefrontal cortex). Critically, this pattern was most pronounced in individuals with PTSD+DS, as compared to both control and PTSD groups. As compared to participants with PTSD and controls, individuals with PTSD+DS showed enhanced pedunculopontine nuclei resting state functional connectivity to the amygdala and the parahippocampal gyrus as well as to the anterior cingulate and the ventromedial prefrontal cortex. No group differences emerged between PTSD and control groups. In individuals with PTSD+DS, state derealization/depersonalization was associated with reduced resting state functional connectivity between the left pedunculopontine nuclei and the anterior nucleus of the thalamus. Altered connectivity in these regions may restrict the thalamo-cortical transmission necessary to integrate internal and external signals at a cortical level and underlie, in part, experiences of depersonalization and derealization.

Conclusions: The present findings extend the current neurobiological model of PTSD and provide emerging evidence for the need to incorporate brainstem structures, including the reticular activation system, into current conceptualizations of PTSD and its dissociative subtype.

[1]Department of Psychiatry, Western University, London, Ontario, Canada
[2]Department of Theoretical Neuroscience, Central Institute of Mental Health Mannheim, Medical Faculty Mannheim, Heidelberg University, Mannheim, Germany
[3]Department of Psychiatry, Central Institute of Mental Health Mannheim, Medical Faculty Mannheim, Heidelberg University, Mannheim, Germany
[4]Imaging Division, Lawson Health Research Institute, London, Ontario, Canada
[5]Department of Neuroscience, Western University, London, Ontario, Canada

[6]Department of Medical Biophysics, Western University, London, Ontario, Canada
[7]Homewood Research Institute, Guelph, Ontario, Canada
[8]Mood Disorder Programs, St. Joseph's Healthcare, Hamilton, Ontario, Canada
[9]Department of Psychiatry and Behavioral Neurosciences, McMaster University, Hamilton, Ontario, Canada

Corresponding Author:
Ruth A. Lanius, Department of Psychiatry, Western University, University Hospital (Room C3-103), 339 Windermere Road, London, Ontario N6A 5A5, Canada.
Email: ruth.lanius@lhsc.on.ca

Introduction

The spontaneous neuronal activation observed during resting state functional magnetic resonance imaging (fMRI) is frequently utilized to illustrate psychopathological alterations in cortical and in subcortical brain networks in psychiatric disorders, serving as a key biomarker in post-traumatic stress disorder (PTSD).[1–14] Importantly, emerging evidence has underscored the importance of incorporating deep-layer midbrain/brainstem neural circuits into the neurobiological framework of PTSD.[1,2,15–19] The reticular activation system (RAS) serves a fundamental role toward the gating of salient, environmental information to higher order, cortical brain structures to facilitate the generation and the maintenance of an arousal state.[20–26] Moreover, the RAS has also been linked to support the formation of action–outcome associations in the brain.[20–26] Hence, the RAS plays a crucial role in supporting reflexive processing, as it shapes the general arousal state of the organism and provides the foundation for innate, defensive responding.[26] Critically, however, prolonged and repeated traumatic experiences may lead to permanent alterations in these fundamental neuronal circuitries.[14,18,27–32]

An important function of the RAS is to promote an arousal state throughout the brain, necessary particularly in the face of immediate danger. The RAS transmits salient information to numerous subcortical and cortical structures, mainly, but not exclusively, via ascending projections through thalamic nuclei (e.g., anterior, medial dorsal, pulvinar nuclei), leading to its identification as "the gatekeeper to consciousness".[33,37] As a result, it has been proposed that the RAS serves a critical role in transitioning between brain states ranging from lower conscious sleep states to states of wakeful presence.[21,38–41] These findings aid greatly in our understanding of PTSD, where PTSD is characterized by frequent shifts in states of arousal, ranging from hyperarousal states, which are more often associated with hypervigilance symptoms, to hypoarousal states, which are more often related to dissociative symptoms (i.e., emotional numbing, depersonalization, derealization); the latter pattern of symptoms is predominant in the recently formulated dissociative subtype.[13,14] Whereas a pattern of decreased brain activation in prefrontal emotion regulatory regions (e.g., ventromedial prefrontal cortex) and increased activation in emotion generating regions (e.g., periaqueductal gray and amygdala) has been associated with hyperarousal,

the opposite pattern of neural activation is indicative of emotional detachment in participants with PTSD and its dissociative subtype, respectively. Notably, this pattern is observed during conditions of both symptom provocation (e.g., traumatic script) and during resting state.[1,2,13–15,17,42–45]

Post-traumatic stress disorder has been further associated with altered threat-related processing, demonstrated by alterations in reaction time, physiological responding (e.g., startle response, heart rate), and the recruitment of brain regions involved in emotion processing (e.g., periaqueductal gray, amygdala) and stimulus evaluation (e.g., inferior orbitofrontal cortex, anterior cingulate cortex) to threat- or trauma-related cues.[5,46–56] Importantly, recent studies emphasize sensitization, particularly in innate threat processing-related brain regions in PTSD, where the presentation of subliminal threat cues elicited stronger activation in the brainstem, the midbrain, the amygdala, and the parahippocampal gyrus in individuals with PTSD as compared to healthy trauma- and non-trauma-exposed controls.[5,57–63]

Despite emerging evidence of altered states of arousal, and the sensitization of innate threat processing in PTSD during symptom provocation and resting state,[1,2,5,43,44,57–62,64–67] research examining connectivity of the RAS to subcortical and to cortical brain structures remains in its nascent stages. Accordingly, we sought to delineate resting state functional connectivity (rsFC) patterns of a main component of the RAS, the pedunculopontine nuclei (PPN),[39,68–75] among individuals with PTSD, its dissociative subtype (PTSD+DS), and healthy controls.

We hypothesized that as compared to controls, both PTSD groups would show altered PPN rsFC to brain regions involved in innate threat processing and arousal (e.g., midbrain, amygdala). Moreover, we hypothesized that individuals with PTSD+DS and PTSD would differ in their PPN rsFC patterns to cortical brain regions involved in emotion regulation (e.g., ventromedial prefrontal cortex).

Methods

Sample Description

The present investigation included 176 participants: 125 participants met the criteria for PTSD and 51 participants were free of any mental disorder throughout their life (control group). Of the 125 participants meeting

criteria for PTSD, 77 individuals met criteria for PTSD without the dissociative subtype and the remaining 48 individuals met criteria for the dissociative subtype of PTSD (PTSD+DS). Details on exclusion criteria can be found in Supplemental Information S1.

Post-traumatic stress disorder diagnoses and symptom severity were assessed using the Clinician-Administered PTSD Scale (CAPS 4, CAPS 5).[76] Comorbid Axis I disorders were diagnosed with the Structured Clinical Interview for DSM-IV Axis I Disorders (SCID-I).[77] Both measures were administered by a trained clinical psychologist.

Childhood traumatization was assessed by the Childhood Trauma Questionnaire (CTQ).[78] The severity of depressive symptomatology and trait dissociation were assessed with the Beck Depression Inventory (BDI)[79] and the Multiscale Dissociation Inventory (MDI),[80] respectively. Immediately after the scanning session was complete, state anxiety (three items of the State-Trait Anxiety Inventory; STAI),[81] and state derealization/depersonalization inventories were administered (Response to Script-Driven Imagery Scale; RSDI). See Supplemental Information S1 for details on statistical analyses.[82]

Scanning took place either at the Robarts Research Institute's Centre for Functional and Metabolic Mapping or the Lawson Health Research Institute for Imaging in London, Ontario, Canada. The study was approved by the research ethics board at Western University of Canada, and all subjects provided written informed consent.

Resting State fMRI Data Acquisition

All fMRI images were collected using a 3.0 T whole-body MRI scanner (Magnetom Tim Trio, Siemens Medical Solutions, Erlangen, Germany) with a manufacturer's 32-channel phased array head coil. T1-weighted anatomical images were collected with 1 mm isotropic resolution [MP-RAGE, TR/TE/TI = 2300 ms/2.98 ms/900 ms, FA 9º, FOV = 256 mm × 240 mm × 192 mm, acceleration factor = 4, total acquisition time = 192 s; (FOV = field of view; TR = time resolution; TE = echotime; FA = flip angle)].

Blood-oxygenation level-dependent signal (BOLD) fMRI images were obtained with the standard gradient-echo planar imaging (EPI) pulse sequence. EPI volumes were acquired with 2 mm isotropic resolution (FOV = 192 mm × 192 mm × 128 mm (94 × 94 matrix, 64 slices), TR/TE = 3000 ms/20 ms, flip angle = 90°, 120 volumes).

Participants were instructed to close their eyes and let their minds wander during the 6-min resting scan.

fMRI Data Preprocessing

Image preprocessing and statistical analyses were conducted using Statistical Parametric Mapping (SPM12,

Wellcome Trust Center of Neuroimaging, London, UK; http://www.fil.ion.ucl.ac.uk/spm) and the spatially unbiased infratentorial template (SUIT) toolbox (version, 3.1)[83] implemented in Matlab R2018b (MathWorks).

The location of the origin of the anatomical images was checked and, in cases of deviation, manually set to the anterior commissure. Functional images were reoriented based on their anatomical image. The 120 (reoriented) functional images were realigned to the first image and resliced to the mean functional image. In addition, six realignment parameters for changes in motion across the different planes were derived. To ensure motion correction, we used the Artifact Detection Tool (ART) software package[84] (at 2 mm motion threshold; ART software; Gabrieli Lab; McGovern Institute for Brain Research, Cambridge, MA; www.nitrc.org/projects/artifact_detect)[84] to compute regressors accounting for motion outlier volumes that were in addition to the six movement regressors computed during standard realignment.

fMRI Data Preprocessing: Brainstem and Cerebellum. To improve the voxel-by-voxel normalization of the midbrain, lower brainstem, and cerebellum and hence, to enhance the depiction and signal extraction of the PPN, functional and anatomical data were normalized to the SUIT template (version 3.1)[83,85] by applying the following steps: (1) whole-brain anatomical images were first segmented and then cropped, retaining only the cerebellum and brainstem; (2) the partial-brain anatomical images were normalized using the SUIT-normalize function that creates a nonlinear deformation map to the SUIT template by applying the cosine-basis approach introduced by Ashburner; (3) the realigned and resliced functional images (see "fMRI Data Preprocessing: Brainstem and Cerebellum" section) were normalized by applying the deformation matrix generated in step 2, cropped (retaining the cerebellum and brainstem only, i.e., functional partial-brain) and resliced to a voxel size of $1.5 \times 1.5 \times 1.5 \, mm^3$; (4) partial-brain functional data were smoothed with a Gaussian filter of 4 mm full-width at half-maximum (FWHM) and band-pass filtered with a high-pass filter of .01 Hz and a low-pass filter of .08 Hz.[86,87]

fMRI Data Preprocessing: Whole Brain. The realigned and resliced functional images (see "fMRI Data Preprocessing" section) were coregistered to the anatomical image for each subject. Coregistration was followed by the segmentation of the images into each tissue type (gray and white matter as well as cerebrospinal fluid), spatial normalization to the Montreal Neurological Institute (MNI) standard template, smoothing with a 6 mm FWHM Gaussian kernel, and band-pass filtering with a high-pass filter of .01 Hz and low-pass filter of .08 Hz.[86,87]

rsFC Analyses

Seed Region Definition. Seed masks for the right and the left PPN were generated using the WFU PickAtlas software (Functional MRI Laboratory, Wake Forest University School of Medicine)[88] by defining 4 mm spheres around the following coordinates: x = ±7, y = −32, z = −22.[89] The seed region was then confirmed visually using Duvernoy's Atlas.[90] Using self-written MATLAB scripts, the mean signal BOLD time course of each seed (i.e., the right and left PPN) was extracted from the partial-brain data, ensuring enhanced spatial accuracy of the defined seed regions (see "fMRI Data Preprocessing: Brainstem and Cerebellum" section).

First Level. For each seed, separate voxel-wise first-level multiple regression models were set up, including the seed time course (i.e., regressor of interest), as well as the ART regressor indicating motion outliers and realignment parameters (i.e., regressors of no interest). Regression analyses were performed at the whole-brain level and separately for the brainstem and the cerebellum, as normalization to the SUIT template allows for increased spatial accuracy at the brainstem/cerebellum level (i.e., partial-brain level).

Second Level: Within-Group Analyses. To explore rsFC patterns of the seed within groups, separate one-sample T-Tests (i.e., right PPN, left PPN) were conducted voxelwise with regard to rsFC at the whole-brain level (see also Tables S4 and S5) as well as at the partial-brain level (Figure 1, Supplemental Information S1; Tables S1 and S2).

Second Level: Between-Group Analyses. To compare rsFC patterns of the PPN between groups, we utilized a flexible-factorial design with the factor group (controls vs. PTSD vs. PTSD+DS) and the factor hemisphere (left PPN vs. right PPN) to test for a significant group × hemisphere interaction with regard to rsFC at the whole-brain level (see also Table S6) and at the partial-brain level (i.e., brainstem/ cerebellum). The latter is included in Supplemental Information only (Table S3).

Second Level: rsFC and Clinical Symptomatology. Multiple regression analyses were conducted to explore the association between rsFC of the seed regions (i.e., right and left PPN) and clinical variables, including PTSD symptom severity (CAPS), childhood traumatization (CTQ), depressive symptomatology (BDI), and state depersonalization/ derealization (RSDI derealization/depersonalization).

Analyses Approach and Statistical Thresholding. Resting state functional connectivity was analyzed using a region-of-interest (ROI) approach, with a priori brain regions, namely, the midbrain, the amygdala, and the ventromedial prefrontal cortex, selected due to their relation to innate threat processing and arousal.[18,19,57,60–63,91–93] We also included the thalamus, as it serves as a major hub in transmitting information from the RAS to cortical and to subcortical structures. Bilateral amygdala, thalamus, and ventromedial prefrontal masks were created with the automated anatomical labeling atlas,[94] which was implemented in the WFU PickAtlas software.[88] A midbrain mask was adopted from the Harvard Ascending Arousal Network (AAN) atlas.[23]

All ROI results were reported at a local significance threshold of $p < .05$ (voxel-level), with an alpha-level adjustment for multiple comparisons (family-wise error (FWE) correction). In addition, a Bonferroni adjustment was applied according to the number of tested ROIs (N = 4), leading to a local significance threshold of $p < .0125$, FWE corrected. Whole-brain results for group differences with a local significance threshold of $p < .001$, $k > 10$, uncorrected for multiple comparisons can be found in the Supplemental Information only (Table S6).

Results

Sociodemographic and Clinical Information

Although groups did not differ in age or gender, significant group differences emerged for all clinical and subjective experience measurements (see Table 1 for details).

PPN Within-Group rsFC

Controls: Left PPN. Controls did not show significant rsFC of the left PPN to any other brain region.

Controls: Right PPN. Controls showed significant rsFC of the right PPN and the right anterior nucleus of the thalamus ($p_{FWE} = .001$) (Figure 2(a)).

PTSD: Left PPN. Individuals with PTSD showed significant rsFC of the left PPN with a cluster encompassing the bilateral anterior, lateral dorsal, and pulvinar nuclei of the thalamus (all $p_{FWE} < .011$), and a cluster encompassing the right anterior cingulate cortex and the ventromedial prefrontal cortex ($p_{FWE} = .004$) (Figure 2(a)).

PTSD: Right PPN. Individuals with PTSD exhibited significant rsFC of the right PPN with a cluster encompassing the bilateral anterior, medial dorsal, lateral dorsal, and pulvinar nuclei of the thalamus (all $p_{FWE} < .001$), a cluster encompassing the left amygdala and the parahippocampal gyrus ($p_{FWE} < .001$), and a cluster encompassing the right anterior cingulate cortex and the ventromedial prefrontal cortex ($p_{FWE} = .005$) (Figure 2(a)).

PTSD+DS: Left PPN. Individuals with PTSD+DS revealed rsFC of the left PPN with a cluster encompassing the

Table 1. Demographic and clinical characteristics of the study sample.

| | Controls N = 51 | PTSD N = 77 | PTSD+DS N = 48 | Test-statistic | p | Post-Hoc Comparison | | | | | | | | |
| | | | | | | Controls vs. PTSD | | | Controls vs. PTSD+DS | | | PTSD vs. PTSD+DS | | |
						Test-statistic	df	p	Test-statistic	df	p	Test-statistic	df	p
Demographics														
Gender (n)														
Female	34	47	39	5.29[a]	.071	—	—	—	—	—	—	—	—	—
Male	17	30	9			—	—	—	—	—	—	—	—	—
Age mean (SD)	35.02 (11.55)	38.82 (11.91)	40.02 (13.59)	2.77[b]	.066	—	—	—	—	—	—	—	—	—
Clinical characteristics														
CAPS total mean (SD)	0.63 (2.72)	56.51 (19.67)	64.09 (22.99)	191.97[b]	<.001*	20.19[c]	125	<.001*	19.57[c]	92	<.001*	1.89[c]	117	.060
MDI				105.88[b]	<.001*									
MDI total mean (SD)	34.04 (3.99)	54.29 (15.09)	81.53 (22.37)			9.25[c]	120	<.001*	14.74[c]	88	<.001*	7.67[c]	110	<.001*
MDI derea mean (SD)	5.22 (0.62)	8.65 (3.28)	13.50 (4.43)			7.31[c]	120	<.001*	13.09[c]	88	<.001*	6.59[c]	110	<.001*
MDI deperso mean (SD)	5.20 (0.64)	6.76 (2.71)	13.05 (5.79)			4.00[c]	120	<.001*	9.52[c]	88	<.001*	7.81[c]	110	<.001*
Trauma history														
CTQ total mean (SD)	32.35 (9.18)	56.82 (22.97)	69.22 (19.64)	46.76[b]	<.001*	7.08[c]	119	<.001*	11.79[c]	91	<.001*	2.98[c]	114	.004*
				5.98[b]	<.001*									
Emotional abuse mean (SD)	6.88 (2.79)	13.94 (6.86)	17.02 (5.49)			6.83[c]	119	<.001*	11.39[c]	91	<.001*	2.52[c]	114	.013
Physical abuse mean (SD)	5.61 (1.55)	9.62 (4.97)	10.23 (4.01)			5.47[c]	119	<.001*	6.25[c]	91	<.001*	0.64[c]	114	.526
Sexual abuse mean (SD)	5.47 (2.12)	9.76 (6.33)	14.02 (7.73)			4.58[c]	119	<.001*	7.44[c]	91	<.001*	3.23[c]	114	.002*
Emotional neglect mean (SD)	8.31 (3.67)	14.24 (6.14)	16.73 (5.08)			6.06[c]	119	<.001*	9.23[c]	91	<.001*	2.26[c]	114	.026
Physical neglect mean (SD)	6.08 (2.14)	9.25 (4.34)	11.23 (4.52)			4.73[c]	119	<.001*	7.13[c]	91	<.001*	2.34[c]	114	.021
Combat exposure[d]				2.63[a]	.269	—	—	—	—	—	—	—	—	—
Yes (N)	3	13	6			—	—	—	—	—	—	—	—	—
No (N)	42	64	42			—	—	—	—	—	—	—	—	—
State characteristics														
RSDI disso mean (SD)	2.74 (0.47)	3.69 (1.36)	4.98 (2.02)	25.69[b]	<.001*	4.66[c]	109	<.001*	7.44[c]	74	<.001*	3.52[c]	87	.001*
STAI-S mean (SD)	3.55 (1.17)	5.75 (2.15)	6.33 (2.43)	28.20[b]	<.001*	6.47[c]	109	<.001*	6.73[c]	74	<.001*	1.16[c]	87	.298

Note: CAPS: Clinician-Administered PTSD Scale; CTQ: Childhood Trauma Questionnaire; Derea: Derealization; Deperso: Depersonalization; MDI: Multiscale Dissociation Inventory; RSDI Disso: Dissociation Items from the Response to Script-Driven Imagery Scale; STAI-S: State-Trait Anxiety Inventory-State part; PTSD: post-traumatic stress disorder, PTSD+DS: PTSD with dissociative subtype;
p: p-value.
[a]Kruskall–Wallis test.
[b]F test.
[c]T Test.
[d]Information is missing for six healthy control individuals.
*Significant at a threshold of p < 0.05, or in case of a significant effect, p-value is Bonferroni-adjusted according to the number of post-hoc comparisons.
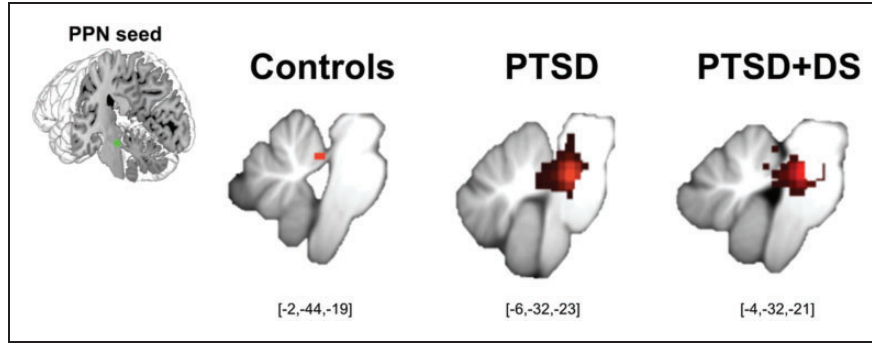
Figure 1. Partial-brain resting state functional connectivity (rsFC) of the left PPN within controls, PTSD, and PTSD+DS separately. RsFC at a local significance threshold of $p < .05$, FWE corrected, partial-brain level (i.e., SUIT space) displayed for each group separately (red color). The seed region (PPN) is displayed in green. Controls exhibited rsFC of the left PPN (within group) with the left cerebellar anterior lobule I to IV only. PTSD exhibited rsFC of the left PPN (within group) with a cluster encompassing the PPN itself, the locus coeruleus, the superior colliculi, the midbrain reticular formation, the left vermis IV to V, and the right cerebellar posterior lobule VI. PTSD+DS exhibited rsFC of the left PPN (within group) with the PPN itself, the locus coeruleus, and the right cerebellar anterior lobule I to IV (see also Tables S1 and S2). PPN: pedunculopontine nuclei; PTSD: post-traumatic stress disorder; PTSD+DS: dissociative subtype of PTSD.
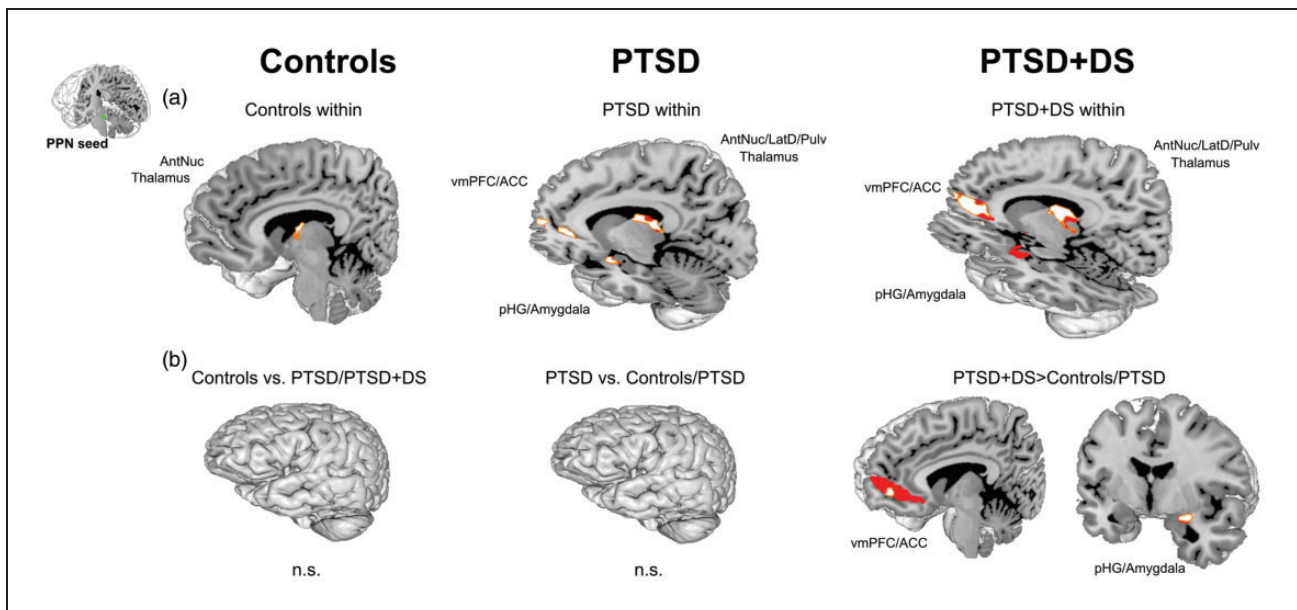

Figure 2. Resting state functional connectivity (rsFC) of the left and right PPN within controls, PTSD, and PTSD+DS separately (a) as well as group comparisons of the left and right PPN (b). ROI approach: rsFC results are reported at a local significance threshold of $p < .0125$, FWE corrected (additionally alpha-level adjustment according to the number of ROIs); only significant voxels surviving the latter threshold are displayed (binary, MNI space). RsFC is displayed in red (a: darker red = left PPN, lighter red = right PPN; b: darker red = PTSD+DS > controls; lighter red = PTSD+DS > PTSD). ACC: anterior cingulate cortex; AntNuc: anterior thalamic nucleus; n.s.: not significant; pHG: parahippocampal gyrus; PPN: pedunculopontine nuclei; PTSD: post-traumatic stress disorder; PTSD+DS: dissociative subtype of PTSD; vmPFC: ventromedial prefrontal cortex.

right anterior, midline, medial dorsal, and lateral dorsal nuclei of the thalamus ($p_{FWE} = .009$), a cluster encompassing the bilateral amygdala and the parahippocampal gyri (all $p_{FWE} < .003$), and a cluster encompassing the right anterior cingulate cortex and the ventromedial prefrontal (all $p_{FWE} < .009$) (Figure 2(a)).

PTSD+DS: Right PPN. Individuals with PTSD+DS were characterized by significant rsFC of the right PPN with a cluster encompassing the right anterior, lateral dorsal, and pulvinar nuclei of the thalamus ($p_{FWE} = .006$), a cluster encompassing the left medial dorsal and pulvinar nuclei of the thalamus ($p_{FWE} = .009$), a cluster

encompassing the bilateral amygdala and the parahippocampal gyri (all $p_{FWE} < .009$), and a cluster encompassing the left anterior cingulate cortex and the ventromedial prefrontal cortex ($p_{FWE} = .012$) (Figure 2(a)).

PPN Between-Group rsFC

The flexible-factorial analysis of variance showed a main effect of group ($p_{FWE} < .018$; alpha-level adjustment with FWE correction, without additional Bonferroni correction). Groups differed in rsFC of the PPN with a cluster encompassing the right amygdala and the parahippocampal gyrus ($p_{FWE} = .014$), and a cluster encompassing the left anterior cingulate cortex and the ventromedial prefrontal cortex ($p_{FWE} = .018$). We did not observe a main effect of hemisphere nor an interaction between the factors group and hemisphere.

Controls Versus PTSD. We did not observe significantly increased rsFC of the PPN with any other brain regions when comparing controls to individuals with PTSD (i.e., controls > PTSD; PTSD > controls).

Controls Versus PTSD+DS. We did not observe significantly stronger rsFC of the PPN with any other brain regions in controls as compared to individuals with PTSD+DS.

Individuals with PTSD+DS as compared to controls exhibited significantly stronger rsFC of the PPN with a cluster encompassing the right amygdala and the parahippocampal gyrus ($p_{FWE} = .010$), and a cluster encompassing the left anterior cingulate and the ventromedial prefrontal cortex ($p_{FWE} = .002$) (Table 2; Figure 2(b)).

PTSD Versus PTSD+DS. We did not observe significantly stronger rsFC of the PPN with any other brain regions in PTSD as compared to PTSD+DS.

Individuals with PTSD+DS as compared to PTSD exhibited significantly stronger rsFC of the PPN with a cluster encompassing the right amygdala and the parahippocampal gyrus ($p_{FWE} = .005$), and a cluster encompassing the left anterior cingulate and the ventromedial prefrontal cortex ($p_{FWE} = .011$) (Table 2; Figure 2(b)).

Relationship Between PPN rsFC and Clinical Characteristics

PTSD. In individuals with PTSD, we did not observe a significant association between rsFC of the PPN and PTSD symptom severity, childhood traumatization, depressive symptomatology, and state derealization/depersonalization.

Table 2. Between-group comparisons of resting state functional connectivity of the left and the right pedunculopontine nuclei.

	L/R	Brain region		k	Z	$p_{FWEcorr}$	p_{uncorr}	Peak MNI coordinate x	y	z
Main effect of group										
	R	Amygdala/parahippocampal gyrus	*	68	3.44	.014	<.001	28	−4	−14
	L	Ventromedial prefrontal/anterior cingulate cortex	*	404	3.61	.018	<.001	−2	50	−12
Main effect of hemisphere										
			n.s.							
Interaction group × hemisphere										
			n.s.							
Between-group comparison										
Controls > PTSD			n.s.							
Controls > PTSD+DS			n.s.							
PTSD > controls			n.s.							
PTSD > PTSD+DS			n.s.							
PTSD+DS > controls	L	Ventromedial prefrontal/anterior cingulate cortex	**	405	4.15	.002	<.001	−2	50	−12
	R	Amygdala/parahippocampal gyrus	**	46	3.50	.010	<.001	28	−4	−14
PTSD+DS > PTSD	L	Ventromedial prefrontal/anterior cingulate cortex	**	172	3.71	.011	<.001	−12	54	−2
	R	Amygdala/parahippocampal gyrus	**	54	3.71	.005	<.001	28	−6	−14

Note: ROI approach: rsFC results are reported at a local significance threshold of *$p < .05$, FWE corrected and **$p < .0125$ (i.e., adjusted for number of ROIs), FWE corrected. PTSD: post-traumatic stress disorder; PTSD+DS: PTSD with the dissociative subtype; L: left; R: right; n.s. = no significant difference; k: cluster size; p_{uncorr}: p-value, uncorrected for multiple comparisons; $p_{FWEcorr}$: p-value, corrected for multiple comparisons (FWE); FWE: family-wise error; MNI: Montreal Neurological Institute.

PTSD+DS. In individuals with PTSD+DS, higher PTSD symptom severity was related to reduced rsFC of the left PPN with the right caudate ($p_{\mathrm{FWE}} = .009$). In addition, in individuals with PTSD+DS, increased state derealization/depersonalization was associated with reduced rsFC of the left PPN with the right anterior nucleus of the thalamus ($p_{\mathrm{FWE}} = .007$) (Table 3; Figure 3). We did not observe a significant relationship between depressive symptomatology or childhood traumatization and rsFC of the PPN and any other brain region in individuals with PTSD+DS.

Discussion

The current investigation aimed to delineate patterns of rsFC with a main component of the RAS, the PPN, a brain region involved in general arousal and innate reflexive responding.[75] Critically, as compared to both controls and PTSD, individuals with PTSD+DS showed increased rsFC of the PPN with a cluster encompassing the amygdala and the parahippocampal gyrus and a cluster encompassing the anterior cingulate and the ventromedial prefrontal cortex, brain regions involved in innate threat processing and arousal.[18,19,91–93,95–97] Among individuals with PTSD, we did not observe differences in PPN rsFC when compared to controls. Interestingly, in individuals with PTSD+DS, increased state derealization/depersonalization was associated with decreased rsFC between the PPN and the anterior nucleus of the thalamus, a pattern that may contribute, in part, to reduced RAS-thalamo-cortical

Table 3. Relationship between resting state functional connectivity of the left pedunculopontine nuclei and clinical characteristics in PTSD+DS individuals.

	PTSD+DS	L/R		Brain region		k	Z	p_{FWEcorr}	p_{uncorr}	Peak MNI Coordinate		
										x	y	z
LPPN	PTSD symptom severity	R	↓	Caudate	**	79	4.38	.009	<.001	4	0	4
	State derealization/depersonalization	R	↓	Thalamus (anterior nucleus)	**	124	4.45	.007	<.001	8	−4	4

ROI approach: rsFC results are reported at a local significance threshold of **$p < .0125$ (i.e., adjusted for number of ROIs), FWE corrected. PTSD: post-traumatic stress disorder; PTSD+DS: PTSD with the dissociative subtype; L: left; R: right; n.s.: no significant difference; k: cluster size; p_{uncorr}: p-value, uncorrected for multiple comparisons; p_{FWEcorr}: p-value, corrected for multiple comparisons (FWE); ↓: negative correlation; FWE: family-wise error; MNI: Montreal Neurological Institute; LPPN: left pedunculopontine nuclei.
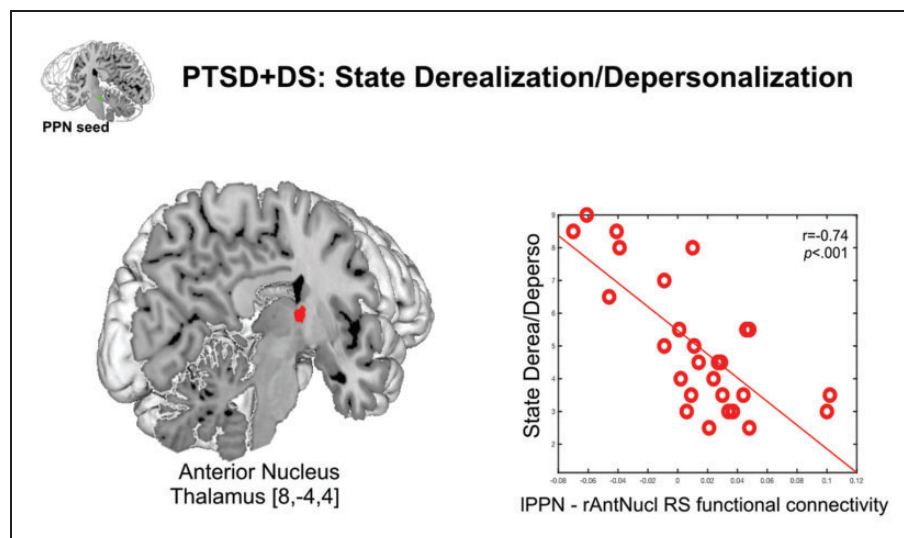

Figure 3. Negative correlation of state depersonalization/derealization with resting state functional connectivity (rsFC) between the left pedunculopontine nucleus and the right thalamus (anterior nucleus) in PTSD+DS. ROI approach: RsFC results are reported at a local significance threshold of $p < .0125$, FWE corrected (additionally adjusted for number of ROIs); only voxels surviving the latter threshold are displayed (binary, MNI space). Correlation with rsFC is displayed in red. The seed region (PPN) is displayed in green. The scatterplot represents the relationship between the extracted beta weights of the rsFC of the lPPN with the right anterior nucleus of the thalamus and state depersonalization/derealization. Derea: derealization; Deperso: depersonalization; lPPN: left pedunculopontine nucleus; rAntNucl: right anterior thalamic nucleus; RS: resting state; PTSD+DS: dissociative subtype of post-traumatic stress disorder; [x, y, z] = [x coordinate, y coordinate, z coordinate].

transmission of interoceptive and exteroceptive signals during states of derealization and depersonalization.[98]

PPN rsFC With Brain Regions Involved in Innate Threat and Arousal Processing

Deep-layer neuronal circuits that control innate and learned reflexive responses as well as arousal[99–101] are becoming increasingly important in the neurobiological conceptualization of PTSD.[1,2,14–16,18,19,65–67,99–103] Crucially, these fundamental neuronal circuits determine the general arousal state of the organism, laying the foundation for reflexive actions.[26] The present investigation provides novel evidence that as compared to both control subjects and individuals with PTSD, participants with PTSD+DS showed stronger rsFC of the PPN with the amygdala, the parahippocampal gyrus, the anterior cingulate cortex, and the ventromedial prefrontal cortex.[91–93,95–97] Taken together, these results reveal increased PPN rsFC to subcortical and cortical brain regions in individuals with PTSD+DS.

Interestingly, the subcortical and the cortical brain regions described above are involved in the innate alarm system, a network of brain regions facilitating "fast-tracked" activation of alerting and defense responses.[91–93,95] Although there is direct communication between deep-layer brain structures of the innate alarm system and cortical brain regions, deep-layer brain regions of the innate alarm system are critical in initiating subliminal, fast responses (i.e., instinctual defense responses via the adaption of physiological arousal), which in turn activate higher level cortical brain regions.[91–93,95–97] Here, we provide the first evidence of increased resting state connectivity between subcortical and cortical components of the innate alarm system and the RAS in individuals with PTSD+DS. This pattern of enhanced connectivity with cortical brain regions may be in keeping with previous observations indicative of cortical top-down regulation of deeper-layer innate alarm system and RAS brain structures in PTSD+DS.[13–15] In addition, enhanced connectivity with the amygdala and the parahippocampal gyrus could indicate modulation of deeper-layer innate alarm regions in PTSD+DS.[62] Further research examining the relation between brainstem, limbic, and cortical neural circuits at rest and in response to symptom provocation is needed urgently.

We did not detect patterns of altered PPN rsFC with any other brain region in PTSD as compared to PTSD+DS and controls. The PPN aids greatly in the integration of incoming sensory information,[41,104,105] a process highly relevant to the clinical model of PTSD+DS, where reduced awareness of the environment and of bodily states characterizes individuals with the dissociative subtype of PTSD. Further research

investigating the heterogeneous neurobiological processes underlying different subtypes of PTSD is needed.

The RAS and Its Relation to Derealization and Depersonalization Experiences

In participants with PTSD+DS, heightened states of derealization/depersonalization were related to reduced rsFC between the PPN and the anterior nucleus of the thalamus. Thalamic nuclei, particularly the anterior, the medial dorsal nuclei, and the pulvinar nuclei, play a pivotal role in controlling intrinsic alertness,[106,107] where intrinsic alertness is defined as a fundamental state of arousal in the absence of any external input. This individual level of intrinsic alertness thus determines readiness to react.[108–111] Critically, states of derealization/depersonalization, that is, psychological defense strategy to trauma, when no physical escape is possible, involve reduced responsiveness to sensory stimuli and hence reduced behavioral action generation,[14] while importantly, this has been associated previously with cortical-sensory deafferentation. Here, the inhibition of the thalamus is stated to restrict the excitation and hence, the somatosensory information transmission to higher order cortical brain structures.[14,98] The present study provides evidence that thalamic engagement (i.e., anterior nucleus) is related to a key RAS brain structure (i.e., PPN).[112] The latter may be critical to establish readiness to react,[71–73,75,106–110] while importantly, this is found to be reduced during states of derealization/depersonalization in PTSD+DS.[14,19,113–122] Hence, as reduced thalamic engagement has been reported repeatedly in PTSD, with most pronounced changes observed in PTSD+DS,[5,123–126] the present investigation extends these findings by highlighting the importance of deep-layer neuronal circuitries in the functioning of higher brain structures involved in depersonalization.

Limitations

There are several limitations to the current investigation. The present investigation was based on 3T fMRI data. As the brainstem comprises relatively small nuclei, future studies using high-resolution fMRI would allow for a more thorough investigation of these nuclei at an enhanced spatial resolution. Task-related studies triggering the RAS specifically would be helpful in gaining further insights into the temporal dynamics of this critical system and the contrasting neural signatures of PTSD and its dissociative subtype.

Conclusion

The present investigation revealed distinct alterations in deep-layer reflexive responding and arousal-related

neuronal circuitries in PTSD and its dissociative subtype during rest. Whereas both PTSD groups exhibited within-group rsFC of the PPN with brain regions implicated in innate threat processing and arousal, as compared to both the control and PTSD groups, only the PTSD+DS group exhibited stronger rsFC of the PPN with a cluster encompassing the amygdala and the para-hippocampal gyrus and a cluster encompassing the anterior cingulate and the ventromedial prefrontal cortex. Taken together, these results highlight the central role of instinctual reflexive responding in PTSD+DS. Critically, in PTSD+DS, increased state derealization/depersonalization was related to reduced PPN and thalamus rsFC, likely reflecting reduced RAS-thalamo-cortical transmission of intero- and exteroceptive signals, thus limiting an individual's perception not only of the condition of one's body but also of one's self in relation to the environment. The latter may serve as an important mechanism underlying depersonalization/derealization. Finally, the present study highlights the necessity of incorporating fundamental brainstem circuitries, including the RAS, into studies seeking to identify the neurobiological underpinnings and clinical characteristics of PTSD and its dissociative subtype.

Declaration of Conflicting Interests

Funding

ORCID iD

Janine Thome https://orcid.org/0000-0002-0215-2097
Braeden Terpou https://orcid.org/0000-0002-6770-2715
Jean Théberge https://orcid.org/0000-0001-7578-4469

Supplemental Material

Supplemental material for this article is available online.

References

1. Harricharan S, Rabellino D, Frewen PA, et al. fMRI functional connectivity of the periaqueductal gray in PTSD and its dissociative subtype. *Brain Behav* 2016; 6(12): e00579.
2. Harricharan S, Nicholson AA, Densmore M, et al. Sensory overload and imbalance: resting-state vestibular connectivity in PTSD and its dissociative subtype. *Neuropsychologia* 2017; 106: 169–178.
3. Barredo J, Aiken E, van't Wout-Frank M, Greenberg BD, Carpenter LL, Philip NS. Network functional architecture and aberrant functional connectivity in post-traumatic stress disorder: a clinical application of network convergence. *Brain Connect* 2018; 8(9): 549–557.
4. Nicholson AA, Densmore M, McKinnon MC, et al. Machine learning multivariate pattern analysis predicts classification of posttraumatic stress disorder and its dissociative subtype: a multimodal neuroimaging approach. *Psychol Med* 2018 [Epub ahead of print]. doi: 10.1017/S0033291718002866.
5. Terpou BA, Densmore M, Theberge J, Frewen P, McKinnon MC, Lanius RA. Resting-state pulvinar-posterior parietal decoupling in PTSD and its dissociative subtype. *Hum Brain Mapp* 2018; 39: 4228–4240.
6. Fu S, Ma X, Wu Y, et al. Altered local and large-scale dynamic functional connectivity variability in posttraumatic stress disorder: a resting-state fMRI study. *Front Psychiatry* 2019; 10: 234.
7. Olson EA, Kaiser RH, Pizzagalli DA, Rauch SL, Rosso IM. Regional prefrontal resting-state functional connectivity in posttraumatic stress disorder. *Biol Psychiatry Cogn Neurosci Neuroimaging* 2019; 4(4): 390–398.
8. Sun D, Phillips RD, Mulready HL, et al. Resting-state brain fluctuation and functional connectivity dissociate moral injury from posttraumatic stress disorder. *Depress Anxiety* 2019; 36(5): 442–452.
9. Weng Y, Qi R, Zhang L, et al. Disturbed effective connectivity patterns in an intrinsic triple network model are associated with posttraumatic stress disorder. *Neurol Sci* 2019; 40(2): 339–349.
10. Zhu H, Li Y, Yuan M, et al. Increased functional segregation of brain network associated with symptomatology and sustained attention in chronic post-traumatic stress disorder. *J Affect Disord* 2019; 247: 183–191.
11. Koch SB, van Zuiden M, Nawijn L, Frijling JL, Veltman DJ, Olff M. Aberrant resting-state brain activity in posttraumatic stress disorder: a meta-analysis and systematic review. *Depress Anxiety* 2016; 33(7): 592–605.
12. Disner SG, Marquardt CA, Mueller BA, Burton PC, Sponheim SR. Spontaneous neural activity differences in posttraumatic stress disorder: a quantitative resting-state meta-analysis and fMRI validation. *Hum Brain Mapp* 2018; 39(2): 837–850.
13. Fenster RJ, Lebois LAM, Ressler KJ, Suh J. Brain circuit dysfunction in post-traumatic stress disorder: from mouse to man. *Nat Rev Neurosci* 2018; 19(9): 535–551.
14. Lanius RA, Boyd JE, McKinnon MC, et al. A review of the neurobiological basis of trauma-related dissociation and its relation to cannabinoid- and opioid-mediated stress response: a transdiagnostic, translational approach. *Curr Psychiatry Rep* 2018; 20(12): 118.
15. Nicholson AA, Friston KJ, Zeidman P, et al. Dynamic causal modeling in PTSD and its dissociative subtype: bottom–up versus top–down processing within fear and emotion regulation circuitry. *Hum Brain Mapp* 2017; 38(11): 5551–5561.
16. Naegeli C, Zeffiro T, Piccirelli M, et al. Locus coeruleus activity mediates hyperresponsiveness in posttraumatic stress disorder. *Biol Psychiatry*. 2018; 83(3): 254–262.

17. Rabellino D, Densmore M, Theberge J, McKinnon MC, Lanius RA. The cerebellum after trauma: resting-state functional connectivity of the cerebellum in posttraumatic stress disorder and its dissociative subtype. *Hum Brain Mapp* 2018; 39(8): 3354–3374.

18. Lanius RA, Rabellino D, Boyd JE, Harricharan S, Frewen PA, McKinnon MC. The innate alarm system in PTSD: conscious and subconscious processing of threat. *Curr Opin Psychol* 2017; 14: 109–115.

19. Terpou BA, Harricharan S, McKinnon MC, Frewen P, Jetly R, Lanius RA. The effects of trauma on brain and body: a unifying role for the midbrain periaqueductal gray. *J Neurosci Res* 2019; 97: 1110–1140.

20. Paus T. Functional anatomy of arousal and attention systems in the human brain. *Prog Brain Res* 2000; 126: 65–77.

21. Parvizi J, Damasio A. Consciousness and the brainstem. *Cognition* 2001; 79(1–2): 135–160.

22. Sarter M, Bruno JP and Berntson GG. Reticular activating-system. In: Nadel L (ed) *Encyclopedia of CognitiveScience: Neuroscience*, vol. 3. London: Nature Publishing Group, 2002, pp. 963–967.

23. Edlow BL, Takahashi E, Wu O, et al. Neuroanatomic connectivity of the human ascending arousal system critical to consciousness and its disorders. *J Neuropathol Exp Neurol* 2012; 71(6): 531–546.

24. Edlow BL, Haynes RL, Takahashi E, et al. Disconnection of the ascending arousal system in traumatic coma. *J Neuropathol Exp Neurol* 2013; 72(6): 505–523.

25. Maldonato M. The ascending reticular activating system. In Esposito A, Bassis S, Morabito FC (eds) *Recent Advances of Neural Network Models and Applications. New York, NY: Springer;* 2014; 333–344.

26. Venkatraman A, Edlow BL, Immordino-Yang MH. The brainstem in emotion: a review. *Front Neuroanat* 2017; 11: 15.

27. Blue AW, Blue MA. The trail of stress. *White Cloud J* 1983; 3(1): 15–22.

28. Pavcovich LA, Ramirez OA. Time course effects of uncontrollable stress in locus coeruleus neuronal activity. *Brain Res Bull* 1991; 26(1): 17–21.

29. Mana M, Grace A. Chronic cold stress alters the basal and evoked electrophysiological activity of rat locus coeruleus neurons. *Neuroscience* 1997; 81(4): 1055–1064.

30. Miyazato H, Skinner RD, Garcia-Rill E. Locus coeruleus involvement in the effects of immobilization stress on the p13 midlatency auditory evoked potential in the rat. *Prog Neuropsychopharmacol Biol Psychiatry* 2000; 24(7): 1177–1201.

31. Perry BD. The neurodevelopmental impact of violence in childhood. In Schetky D and Benedek EP (eds) *Textbook of Child and Adolescent Forensic Psychiatry*. Washington, DC: American Psychiatric Press, Inc, 2001, pp. 221–238.

32. George SA, Knox D, Curtis AL, Aldridge JW, Valentino RJ, Liberzon I. Altered locus coeruleus–norepinephrine function following single prolonged stress. *Eur J Neurosci* 2013; 37(6): 901–909.

33. Garcia-Rill E. Disorders of the reticular activating system. *Med Hypotheses* 1997; 49(5): 379–387.

34. Jang SH, Kwon HG. The direct pathway from the brainstem reticular formation to the cerebral cortex in the ascending reticular activating system: a diffusion tensor imaging study. *Neurosci Lett* 2015; 606: 200–203.

35. Mikolajewska E, Mikolajewski D. Consciousness disorders as the possible effect of brainstem activity failure—computational approach. *J Health Sci* 2012; 2(2): 007–18.

36. Moruzzi G, Magoun HW. Brain stem reticular formation and activation of the EEG. *Electroencephalogr Clin Neurophysiol* 1949; 1(1–4): 455–473.

37. Yao S, Qi S, Kendrick KM, Mobbs D. Attentional set to safety recruits the ventral medial prefrontal cortex. *Sci Rep* 2018; 8(1): 15395.

38. Steriade M. Arousal: revisiting the reticular activating system. *Science* 1996; 272(5259): 225–226.

39. Steriade M. Awakening the brain. *Nature* 1996; 383(6595): 24–25.

40. Datta S, Siwek DF. Single cell activity patterns of pedunculopontine tegmentum neurons across the sleep-wake cycle in the freely moving rats. *J Neurosci Res* 2002; 70(4): 611–621.

41. Steriade MM, McCarley RW. *Brainstem Control of Wakefulness and Sleep*. New York, NY: Springer; 2013.

42. Thomaes K, Dorrepaal E, Draijer NP, et al. Increased activation of the left hippocampus region in Complex PTSD during encoding and recognition of emotional words: a pilot study. *Psychiatry Res* 2009; 171(1): 44–53.

43. Melara RD, Ruglass LM, Fertuck EA, Hien DA. Regulation of threat in post-traumatic stress disorder: associations between inhibitory control and dissociative symptoms. *Biol Psychol* 2018; 133: 89–98.

44. Rabellino D, Densmore M, Harricharan S, Jean T, McKinnon MC, Lanius RA. Resting-state functional connectivity of the bed nucleus of the stria terminalis in post-traumatic stress disorder and its dissociative subtype. *Hum Brain Mapp* 2018; 39(3): 1367–1379.

45. Weston CS. Posttraumatic stress disorder: a theoretical model of the hyperarousal subtype. *Front Psychiatry* 2014; 5: 37.

46. McNally RJ, Kaspi SP, Riemann BC, Zeitlin SB. Selective processing of threat cues in posttraumatic stress disorder. *J Abnorm Psychol* 1990; 99(4): 398.

47. Foa EB, Feske U, Murdock TB, Kozak MJ, McCarthy PR. Processing of threat-related information in rape victims. *J Abnorm Psychol* 1991; 100(2): 156.

48. Cassiday KL, McNally RJ, Zeitlin SB. Cognitive processing of trauma cues in rape victims with post-traumatic stress disorder. *Cognit Ther Res* 1992; 16(3): 283–295.

49. Ashley V, Honzel N, Larsen J, Justus T, Swick D. Attentional bias for trauma-related words: exaggerated emotional Stroop effect in Afghanistan and Iraq war veterans with PTSD. *BMC Psychiatry* 2013; 13(1): 86.

50. Martinson AA, Sigmon ST, Craner J, Rothstein E, McGillicuddy M. Processing of intimacy-related stimuli in survivors of sexual trauma: the role of PTSD. *J Interpers Violence* 2013; 28(9): 1886–1908.

51. Lang PJ, McTeague LM, Bradley MM. RDoC, DSM, and the reflex physiology of fear: a biodimensional analysis of the anxiety disorders spectrum. *Psychophysiology* 2016; 53(3): 336–347.

52. Zuj DV, Palmer MA, Gray KE, et al. Negative appraisals and fear extinction are independently related to PTSD symptoms. *J Affect Disord* 2017; 217: 246–251.

53. Thome J, Hauschild S, Koppe G, et al. Generalisation of fear in PTSD related to prolonged childhood maltreatment: an experimental study. *Psychol Med* 2018; 48(13): 2223–2234.

54. Fani N, King TZ, Clendinen C, et al. Attentional control abnormalities in posttraumatic stress disorder: Functional, behavioral, and structural correlates. *J Affect Disord* 2019; 253: 343–351.

55. Herzog S, D'Andrea W, DePierro J. Zoning out: automatic and conscious attention biases are differentially related to dissociative and post-traumatic symptoms. *Psychiatry Res* 2019; 272: 304–310.

56. Powers A, Fani N, Murphy L, et al. Attention bias toward threatening faces in women with PTSD: eye tracking correlates by symptom cluster. *Eur J Psychotraumatol* 2019; 10(1): 1568133.

57. Rauch SL, Whalen PJ, Shin LM, et al. Exaggerated amygdala response to masked facial stimuli in posttraumatic stress disorder: a functional MRI study. *Biol Psychiatry* 2000; 47(9): 769–776.

58. Hendler T, Rotshtein P, Yeshurun Y, et al. Sensing the invisible: differential sensitivity of visual cortex and amygdala to traumatic context. *NeuroImage.* 2003; 19(3): 587–600.

59. Sakamoto H, Fukuda R, Okuaki T, et al. Parahippocampal activation evoked by masked traumatic images in posttraumatic stress disorder: a functional MRI study. *NeuroImage* 2005; 26(3): 813–821.

60. Bryant RA, Kemp AH, Felmingham KL, et al. Enhanced amygdala and medial prefrontal activation during nonconscious processing of fear in posttraumatic stress disorder: an fMRI study. *Hum Brain Mapp* 2008; 29(5): 517–523.

61. Felmingham K, Kemp AH, Williams L, et al. Dissociative responses to conscious and non-conscious fear impact underlying brain function in post-traumatic stress disorder. *Psychol Med* 2008; 38(12): 1771–1780.

62. Kemp AH, Felmingham KL, Falconer E, Liddell BJ, Bryant RA, Williams LM. Heterogeneity of non-conscious fear perception in posttraumatic stress disorder as a function of physiological arousal: an fMRI study. *Psychiatry Res* 2009; 174(2): 158–161.

63. Neumeister P, Feldker K, Heitmann CY, et al. Specific amygdala response to masked fearful faces in posttraumatic stress relative to other anxiety disorders. *Psychol Med* 2018; 48(7): 1209–1217.

64. Brown VM, LaBar KS, Haswell CC, et al. Altered resting-state functional connectivity of basolateral and centromedial amygdala complexes in posttraumatic stress disorder. *Neuropsychopharmacology* 2014; 39(2): 361.

65. Steuwe C, Daniels JK, Frewen PA, et al. Effect of direct eye contact in PTSD related to interpersonal trauma: an fMRI study of activation of an innate alarm system. *Soc Cogn Affect Neurosci* 2014; 9(1): 88–97.

66. Rabellino D, Densmore M, Frewen PA, Theberge J, Lanius RA. The innate alarm circuit in post-traumatic stress disorder: conscious and subconscious processing of fear- and trauma-related cues. *Psychiatry Res Neuroimaging* 2016; 248: 142–150.

67. Terpou BA, Densmore M, Thome J, Frewen P, McKinnon MC, Lanius RA. The innate alarm system and subliminal threat presentation in posttraumatic stress disorder: neuroimaging of the midbrain and cerebellum. *Chronic Stress* 2019; 3: 2470547018821496.

68. Garcia-Rill E. The pedunculopontine nucleus. *Prog Neurobiol* 1991; 36(5): 363–389.

69. Kinomura S, Larsson J, Gulyas B, Roland PE. Activation by attention of the human reticular formation and thalamic intralaminar nuclei. *Science* 1996; 271(5248): 512–515.

70. Kobayashi Y, Isa T. Sensory-motor gating and cognitive control by the brainstem cholinergic system. *Neural Netw* 2002; 15(4–6): 731–741.

71. Benarroch EE. Pedunculopontine nucleus: functional organization and clinical implications. *Neurology* 2013; 80(12): 1148–1155.

72. Garcia-Rill E, D'Onofrio S, Mahaffey S. Bottom-up gamma: the pedunculopontine nucleus and reticular activating system. *Transl Brain Rhythm* 2016; 1(2): 49.

73. Goetz L, Piallat B, Bhattacharjee M, Mathieu H, David O, Chabardès S. On the role of the pedunculopontine nucleus and mesencephalic reticular formation in locomotion in nonhuman primates. *J Neurosci* 2016; 36(18): 4917–4929.

74. Gut NK, Winn P. The pedunculopontine tegmental nucleus—a functional hypothesis from the comparative literature. *Mov Disord* 2016; 31(5): 615–624.

75. Mena-Segovia J, Bolam JP. Rethinking the pedunculopontine nucleus: from cellular organization to function. *Neuron* 2017; 94(1): 7–18.

76. Blake DD, Weathers FW, Nagy LM, et al. The development of a Clinician-Administered PTSD Scale. *J Trauma Stress* 1995; 8(1): 75–90.

77. First MB, Spitzer RL, Gibbon M, Williams JB, eds. *Structured Clinical Interview for DSM IV Axis I Disorders*, Research Version, Non-patient Edition (SCID - I/NP). New York, NY: Biometrics Research, 2002.

78. Bernstein DP, Stein JA, Newcomb MD, et al. Development and validation of a brief screening version of the Childhood Trauma Questionnaire. *Child Abuse Negl* 2003; 27(2): 169–190.

79. Beck AT, Guth D, Steer RA, Ball R. Screening for major depression disorders in medical inpatients with the Beck Depression Inventory for Primary Care. *Behav Res Ther* 1997; 35(8): 785–791.

80. Briere J, Weathers FW, Runtz M. Is dissociation a multidimensional construct? Data from the Multiscale Dissociation Inventory. *J Trauma Stress* 2005; 18(3): 221–231.

81. Spielberger CD. *State-Trait Anxiety Inventory. The Corsini Encyclopedia of Psychology.* Hoboken, NJ: John Wiley, 2010.

82. Hopper JW, Frewen PA, Van der Kolk BA, Lanius RA. Neural correlates of reexperiencing, avoidance, and dissociation in PTSD: Symptom dimensions and emotion dysregulation in responses to script-driven trauma imagery. *J Trauma Stress* 2007; 20(5): 713–725.

83. Diedrichsen J. A spatially unbiased atlas template of the human cerebellum. *NeuroImage* 2006; 33(1): 127–138.

84. Power JD, Barnes KA, Snyder AZ, Schlaggar BL, Petersen SE. Spurious but systematic correlations in functional connectivity MRI networks arise from subject motion. *NeuroImage* 2012; 59(3): 2142–2154.

85. Diedrichsen J, Maderwald S, Küper M, et al. Imaging the deep cerebellar nuclei: a probabilistic atlas and normalization procedure. *NeuroImage* 2011; 54(3): 1786–1794.

86. Bär KJ, de la Cruz F, Schumann A, et al. Functional connectivity and network analysis of midbrain and brainstem nuclei. *Neuroimage* 2016; 134: 53–63.

87. Wagner G, Krause-Utz A, de la Cruz F, Schumann A, Schmahl C, Bar KJ. Resting-state functional connectivity of neurotransmitter producing sites in female patients with borderline personality disorder. *Prog Neuropsychopharmacol Biol Psychiatry* 2018; 83: 118–126.

88. Maldjian JA, Laurienti PJ, Kraft RA, Burdette JH. An automated method for neuroanatomic and cytoarchitectonic atlas-based interrogation of fMRI data sets. *NeuroImage* 2003; 19(3): 1233–1239.

89. Fling BW, Cohen RG, Mancini M, Nutt JG, Fair DA, Horak FB. Asymmetric pedunculopontine network connectivity in parkinsonian patients with freezing of gait. *Brain* 2013; 136(8): 2405–2418.

90. Naidlich T. *Duvernoy's Atlas of the Human Brain Stem and Cerebellum*. Vienna, Austria: Springer.

91. Williams LM, Liddell BJ, Rathjen J, et al. Mapping the time course of nonconscious and conscious perception of fear: An integration of central and peripheral measures. *Hum Brain Mapp* 2004; 21(2): 64–74.

92. Liddell BJ, Brown KJ, Kemp AH, et al. A direct brainstem-amygdala-cortical 'alarm' system for subliminal signals of fear. *NeuroImage*. 2005; 24(1): 235–243.

93. Williams LM, Liddell BJ, Kemp AH, et al. Amygdala–prefrontal dissociation of subliminal and supraliminal fear. *Hum Brain Mapp* 2006; 27(8): 652–661.

94. Tzourio-Mazoyer N, Landeau B, Papathanassiou D, et al. Automated anatomical labeling of activations in SPM using a macroscopic anatomical parcellation of the MNI MRI single-subject brain. *NeuroImage* 2002; 15(1): 273–289.

95. Phillips ML, Williams LM, Heining M, et al. Differential neural responses to overt and covert presentations of facial expressions of fear and disgust. *NeuroImage* 2004; 21(4): 1484–1496.

96. Garvert MM, Friston KJ, Dolan RJ, Garrido MI. Subcortical amygdala pathways enable rapid face processing. *NeuroImage* 2014; 102: 309–316.

97. Morawetz C, Bode S, Baudewig J, Heekeren HR. Effective amygdala-prefrontal connectivity predicts individual differences in successful emotion regulation. *Soc Cogn Affect Neurosci* 2017; 12(4): 569–585.

98. Schauer M, Elbert T. Dissociation following traumatic stress. *J Psychol* 2010; 218(2): 109–127.

99. LeDoux J, Daw ND. Surviving threats: Neural circuit and computational implications of a new taxonomy of defensive behaviour. *Nat Rev Neurosci* 2018; 19(5): 269.

100. Qi S, Hassabis D, Sun J, Guo F, Daw N, Mobbs D. How cognitive and reactive fear circuits optimize escape decisions in humans. *Proc Natl Acad Sci U S A* 2018; 115(12): 3186–3191.

101. Reddan MC, Wager TD, Schiller D. Attenuating neural threat expression with imagination. *Neuron* 2018; 100(4): 994–1005.e4.

102. Rabellino D, D'Andrea W, Siegle G, et al. Neural correlates of heart rate variability in PTSD during sub- and supraliminal processing of trauma-related cues. *Hum Brain Mapp* 2017; 38(10): 4898–4907.

103. Olive I, Densmore M, Harricharan S, Theberge J, McKinnon MC, Lanius R. Superior colliculus resting state networks in post-traumatic stress disorder and its dissociative subtype. *Hum Brain Mapp* 2018; 39(1): 563–574.

104. Garcia-Rill E, Luster B, Mahaffey S, Bisagno V, Urbano FJ. Pedunculopontine arousal system physiology—implications for insomnia. *Sleep Sci* 2015; 8(2): 92–99.

105. Sharma VD, Sengupta S, Chitnis S, Amara AW. Deep brain stimulation and sleep-wake disturbances in Parkinson disease: A review. *Front Neurol* 2018; 9: 697.

106. Clemens B, Zvyagintsev M, Sack A, Heinecke A, Willmes K, Sturm W. Revealing the functional neuroanatomy of intrinsic alertness using fMRI: Methodological peculiarities. *PLoS One* 2011; 6(9): e25453.

107. Mottaghy FM, Willmes K, Horwitz B, Müller H-W, Krause BJ, Sturm W. Systems level modeling of a neuronal network subserving intrinsic alertness. *NeuroImage* 2006; 29(1): 225–233.

108. Posner MI, Petersen SE. The attention system of the human brain. *Annu Rev Neurosci* 1990; 13(1): 25–42.

109. Posner MI, Rothbart MK. Attentional mechanisms and conscious experience. In Milner AD and Rugg MD (eds) *The Neuropsychology of Consciousness*. Amsterdam, the Netherlands: Elsevier; 1992 91.

110. Sturm W, De Simone A, Krause B, et al. Functional anatomy of intrinsic alertness: Evidence for a fronto-parietal-thalamic-brainstem network in the right hemisphere. *Neuropsychologia* 1999; 37(7): 797–805.

111. Sturm W, Willmes K. On the functional neuroanatomy of intrinsic and phasic alertness. *NeuroImage* 2001; 14(1): S76–S84.

112. Holmstrand EC, Sesack SR. Projections from the rat pedunculopontine and laterodorsal tegmental nuclei to the anterior thalamus and ventral tegmental area arise from largely separate populations of neurons. *Brain Struct Funct* 2011; 216(4): 331–345.

113. Bovin MJ, Jager-Hyman S, Gold SD, Marx BP, Sloan DM. Tonic immobility mediates the influence of peritraumatic fear and perceived inescapability on posttraumatic stress symptom severity among sexual assault survivors. *J Trauma Stress* 2008; 21(4): 402–409.

114. Fiszman A, Mendlowicz MV, Marques-Portella C, et al. Peritraumatic tonic immobility predicts a poor response to pharmacological treatment in victims of urban violence with PTSD. *J Affect Disord* 2008; 107(1-3): 193–197.

115. Lima AA, Fiszman A, Marques-Portella C, et al. The impact of tonic immobility reaction on the prognosis of posttraumatic stress disorder. *J Psychiatr Res* 2010; 44(4): 224–228.

116. Fani N, King TZ, Powers A, et al. Cognitive and neural facets of dissociation in a traumatized population. *Emotion* 2019; 19: 863–875.

117. Rabellino D, Burin D, Harricharan S, et al. Altered sense of body ownership and agency in posttraumatic stress disorder and its dissociative subtype: A rubber hand illusion study. *Front Human Neurosci* 2018; 12: 163.

118. Seligowski AV, Lebois LAM, Hill SB, et al. Autonomic responses to fear conditioning among women with PTSD and dissociation. *Depress Anxiety* 2019; 36: 625–634.

119. Gjini K, Boutros NN, Haddad L, et al. Evoked potential correlates of post-traumatic stress disorder in refugees with history of exposure to torture. *J Psychiatr Res* 2013; 47(10): 1492–1498.

120. Dong X, Li Y. Peritraumatic startle response predicts the vulnerability to develop PTSD-like behaviors in rats: A model for peritraumatic dissociation. *Front Behav Neurosci* 2014; 8: 14.

121. Maia DB, Nobrega A, Marques-Portella C, et al. Peritraumatic tonic immobility is associated with PTSD symptom severity in Brazilian police officers: A prospective study. *Braz J Psychiatry*. 2015; 37(1): 49–54.

122. TeBockhorst SF, O'Halloran MS, Nyline BN. Tonic immobility among survivors of sexual assault. *Psychol Trauma* 2015; 7(2): 171–178.

123. Kim SJ, Lyoo IK, Lee YS, et al. Decreased cerebral blood flow of thalamus in PTSD patients as a strategy to reduce re-experience symptoms. *Acta Psychiatr Scand* 2007; 116(2): 145–153.

124. Lanius RA, Williamson PC, Densmore M, et al. Neural correlates of traumatic memories in posttraumatic stress disorder: A functional MRI investigation. *Am J Psychiatry* 2001; 158(11): 1920–1922.

125. Lanius RA, Williamson PC, Hopper J, et al. Recall of emotional states in posttraumatic stress disorder: An fMRI investigation. *Biol Psychiatry* 2003; 53(3): 204–210.

126. Yan X, Brown AD, Lazar M, et al. Spontaneous brain activity in combat related PTSD. *Neurosci Lett* 2013; 547: 1–5.